M.J. Hornos et al. (Eds.)

doi:10.3233/AISE240024

# Evaluation of Pre-Trained CNN Models for 2D Image-Based Drug Discovery

Antonio Jesus BANEGAS-LUNA [a,1], and Juan BONASTRE-EGEA [b]
[a] *BIO-HPC, Universidad Católica de Murcia (UCAM), Murcia, Spain*
[b] *UKEIM, Universidad Católica de Murcia (UCAM), Murcia, Spain*
ORCiD ID: Antonio Jesus Banegas-Luna https://orcid.org/0000-0003-1158-8877, Juan Bonastre-Egea https://orcid.org/0009-0002-9633-8454

**Abstract.** Recent advancements in computer-aided drug discovery revolutionize healthcare by integrating virtual screening (VS) and artificial intelligence (AI). Virtual screening enables the efficient screening of vast chemical libraries *in silico*, reducing the number of compounds requiring physical testing in the lab before drug synthesis or repurposing. An essential aspect of successful virtual screening is the representation of chemical compounds. While traditionally represented as feature vectors, leveraging convolutional neural networks (CNNs) to interpret chemical structures as images has emerged as a promising approach, harnessing the learning capabilities of CNNs. One potential application of CNNs is in creating classifiers capable of accurately distinguishing between drugs and decoys. These classifiers could serve as a foundation for developing generative adversarial neural networks (GANs), facilitating the synthetic generation of potential non-toxic drugs. This study, which attempts to serve as a basis for future work in the field of smart health, assesses a selection of pre-trained CNNs for their efficacy in classifying drugs associated with diabetes, cancer, and malaria. To enhance model training, a data augmentation phase has been incorporated, introducing variations to the initial images to impart rotational invariance to the learning process. Results indicate that DenseNet201 exhibits superior accuracy, albeit with considerable computational time requirements. Surprisingly, excluding data augmentation significantly improves predictive performance across all models, challenging the initial assumptions. Consequently, applying pre-trained CNNs for drug classification is contingent upon specific conditions, necessitating carefully considering augmentation strategies for optimal outcomes.

**Keywords.** computer-aided drug discovery, convolutional neural network, deep learning, image processing, data augmentation, generative adversarial networks

## 1. Introduction

Intelligent environments, such as smart homes or smart cities, leverage artificial intelligence (AI) to enhance various aspects of living, from energy efficiency to healthcare [1,2]. AI-based drug discovery can significantly contribute to intelligent environments in several ways. One of these ways is drug repositioning, which consists of using drugs approved and validated in certain diseases to treat others [3]. AI can analyze existing

[1] Corresponding Author: Antonio Jesus Banegas-Luna, ajbanegas@ucam.edu.

drugs and their mechanisms of action to identify new therapeutic uses [4,5,6]. In intelligent environments, this capability can lead to the discovery of novel disease treatments more efficiently and cost-effectively by repurposing drugs that have already undergone extensive testing for safety. Moreover, AI can design and optimize drug delivery systems tailored to individual patient needs [7,8] that could involve smart drug delivery devices that administer medications at optimal times and doses, improving treatment outcomes and patient adherence. Overall, AI-based drug discovery holds great promise for enhancing healthcare in intelligent environments by enabling personalized treatments, early disease detection, optimized clinical trials, drug repurposing, environmental monitoring, optimized drug delivery, and continuous monitoring and feedback.

Computational techniques, such as virtual screening (VS), dramatically accelerate drug repurposing. VS is a collection of computational techniques to identify the most promising drug candidates among the existing compounds in chemical databases [9]. Among the VS approaches, shape similarity is the preferred one when the tri-dimensional structure of the target is unknown but a database of small molecules, called *ligands*, is available. Shape similarity relies on the similarity principle, which states that two structurally similar compounds can show the same biological activity [10]. Usually, the similarity between two compounds is calculated with mathematical tools like the Euclidean distance. This is possible because the compounds can be depicted as numerical vectors of features, called *descriptors*.

How compounds are represented strongly determines what kind of AI models can be used for certain tasks. For example, graph-based neural networks (GNNs) allow the manipulation of compounds through their coordinates in three-dimensional space. This representation is suitable for tasks like predicting drug-target interactions [11] and de-novo drug design [12]. Alphafold [13] revolutionalized the prediction of proteins' structure by incorporating genetic information into a deep neural network. The model profits from the fact that proteins can be represented in FASTA format to outperform the state-of-the-art dramatically. Chemical compounds can also be represented graphically like images, feeding convolutional neural networks (CNN). CNNs have been extensively studied in the context of drug discovery. Their main usage has been as scoring functions in molecular docking calculations [14,15], which is a technique that relies on the 3D structure of the target to predict the best pose and placement of a ligand on a target receptor. Qian et al. [16] implemented an advanced transformer model and a CNN for predicting compound-protein interactions. CNNs have also been employed in different tasks based on the SMILES (Simplified Molecular Input Line Entry Specification) representation of the chemical compounds. SMILES is a textual representation that can be easily depicted as a matrix that CNNs can process [17,18]. Both CNNs and GNNs can be combined in the same architecture. Mendolia et al. [19] developed a GNN-based tool for representing chemical compounds. This type of architecture leverages that compounds can be represented in the tri-dimensional space by their coordinates, which makes it easy to manipulate by GNNs. The extensive use of CNNs has also led to the development of generative adversarial networks (GAN) for different drug discovery tasks [20,21,22]. Unfortunately, because of their toxicity, synthetic chemical compounds generated with GANs barely pass *in-vivo* tests. To overcome this problem, accurate classifiers capable of discriminating between approved and toxic drugs would be needed.

This work evaluates a diversity of pre-trained CNN models as potential non-toxic drug classifiers. The models have been trained with three *in-house* datasets containing

approved drugs for diabetes, cancer, and malaria. Typical classification metrics, such as precision, recall, F1 score, and the area under the curve (AUC), have been used to assess the models. Additionally, the training times have been measured. The potential drugs and their corresponding decoys have been transformed from SMILES format to 2D images representing their structure. A data augmentation process has been implemented to enhance the learning of the models. The input images have been carefully flipped and rotated to make the model learn the drugs in different positions.

The next section describes the three datasets and the CNN models employed in the experiment. In section 3, the collected metrics and main results are presented. Next, the reasons behind the results are disclosed in section 4. Finally, the main conclusions and future works are summarized in section 5.

## 2. Materials and Methods

### 2.1. Datasets

Three datasets of established drugs for diabetes, cancer, and malaria were utilized to benchmark the models. These datasets were selected for their well-known and publicly available compounds. Choosing datasets with poorly validated drugs could have hindered the models' ability to discriminate appropriate compounds, leading to invalid results. The required compounds have been collected in SMILES format and converted to 2D images with the Open Babel tool [23]. Anti-diabetic compounds were collected from an *in-house* database which is available for VS purposes [24]. In a previous paper, Mswahili et al. [25] reported an extensive antimalarial drug list. A subset of the published drug list has been used for training the CNN models. Finally, the anticancer drugs were collected from [26], where the authors present a detailed subclassification of anticancer drugs. In our work, the compounds were all labeled as cancer inhibitors. The three datasets were completed with random decoys, which are compounds not showing the same biological activity as the drugs. Such decoys were randomly extracted from DrugBank 5 [27] and ChEMBL 33 databases [28]. As many decoys as inhibitors were added to keep the dataset balanced and facilitate the learning of models (Table 1).

**Table 1.** Number of training and validation samples of the three datasets.

| | Training | | Validation | |
|---|---|---|---|---|
| **Dataset** | **Drugs** | **Decoys** | **Drugs** | **Decoys** |
| Diabetes | 149 | 149 | 37 | 37 |
| Cancer | 42 | 42 | 11 | 11 |
| Malaria | 300 | 300 | 75 | 75 |

### 2.2. CNN Models

Ten pre-trained CNN models have been evaluated: VGG16 [29], VGG19 [29], ResNet50V2 [30], ResNet101 [30], DenseNet201 [31], InceptionV3 [32], Xception [33], MobileNetV2 [34], EfficientNetV2B3 [35] and AlexNet [36]. The implementation of the AlexNet model was inferred from the original paper [37], while the other models are

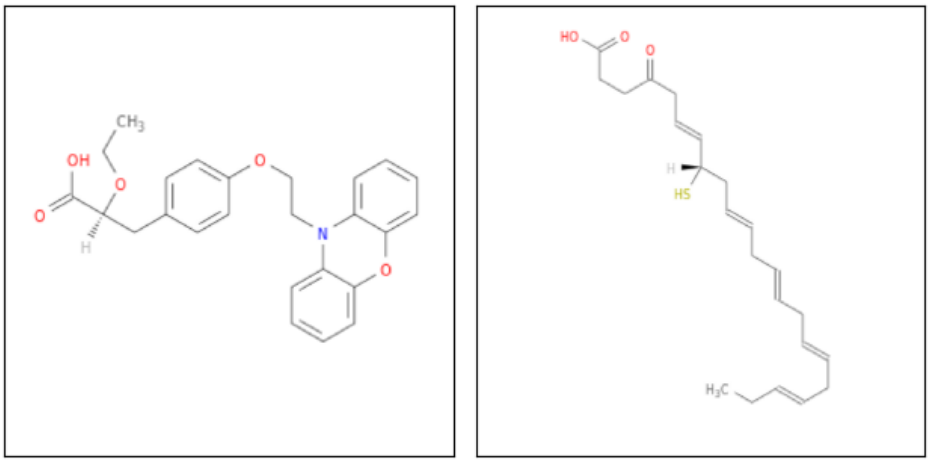


**Figure 1.** Examples of synthetically generated images for the diabetes dataset.

implemented in Tensorflow 2.15. The convolutional layers were completed with two Dense layers of 4096 units and *relu* activation. A Dropout layer with a rate of 20% followed the second dense layer. Aiming to apply the transfer learning approach, the models were initialized with the ImageNet [38] weights, and the input images were reshaped to 224x224. The models were evaluated for accuracy, precision, recall, F1 score, and AUC metrics. In this work, the AUC will be the reference metric for choosing the best model. Additionally, the training time was taken. An Adam optimizer with a learning rate of 0.0001 was used. The assessed models were selected based on the Keras performance metrics for models trained with the ImageNet weights. A range of models with diverse depths was selected, and a trade-off between accuracy, speed, and memory consumption was intended to select the versions. All the models reported accuracy higher than 90% in classification tasks, and their inference time on GPU was less than 8 seconds [39].

## 3. Results

Due to the small datasets, augmentation was done to create more images. This involved rotating images up to 180º and flipping them horizontally and vertically. Pixel values were scaled in the range (1, 255) for stability. Brightness was adjusted without altering compound notation. Minimal zoom (0.05 range) was applied to avoid structural distortion. Augmented images were used for training and validation. See Figure 1 for examples of new anti-diabetics.

The models were first trained for 20 epochs, and the weights of the best epoch were saved for later. Fine-tuning was then applied by freezing a variable number of layers. As the evaluated models had different depths, 70% of the lower layers were frozen, and the rest were trained for 10 additional epochs starting with the previously saved weights. Finally, the models were evaluated 30 times each to avoid bias in the metrics. The training and evaluation process was repeated 10 times, and the metrics were averaged. The calculations were carried out on an NVIDIA GeForce RTX 3090 GPU. Table 2 summarizes the average AUC of each model with and without data augmentation. Finally, Table 3 shows the training process's computing times along with the datasets' main features.

**Table 2.** Average AUC of each model with and without data augmentation for the three datasets.

| Model | Diabetes | | Cancer | | Malaria | |
|---|---|---|---|---|---|---|
| | Aug. | No Aug. | Aug. | No Aug. | Aug. | No Aug. |
| VGG16 | **0.741±0.04** | **0.993±0.01** | 0.688±0.03 | 0.889±0.24 | 0.627±0.02 | 0.813±0.03 |
| VGG19 | 0.732±0.03 | 0.730±0.08 | 0.678±0.03 | 0.194±0.10 | 0.612±0.02 | 0.769±0.02 |
| ResNet50V2 | 0.638±0.02 | 0.599±0.07 | 0.604±0.06 | 0.500±0.00 | 0.591±0.03 | 0.530±0.15 |
| ResNet101 | 0.611±0.07 | 0.732±0.10 | 0.527±0.03 | 0.750±0.00 | 0.497±0.01 | **0.906±0.06** |
| DenseNet201 | 0.710±0.07 | 0.782±0.11 | 0.764±0.06 | 0.472±0.25 | 0.673±0.02 | 0.691±0.10 |
| InceptionV3 | 0.662±0.04 | 0.645±0.10 | **0.795±0.03** | 0.694±0.20 | 0.663±0.03 | 0.759±0.13 |
| Xception | 0.621±0.06 | 0.710±0.17 | 0.710±0.09 | 0.375±0.32 | 0.635±0.05 | 0.613±0.11 |
| MobileNetV2 | 0.721±0.04 | 0.760±0.05 | 0.671±0.05 | 0.250±0.00 | **0.691±0.03** | 0.648±0.03 |
| EfficientNetV2B3 | 0.507±0.02 | 0.710±0.07 | 0.496±0.02 | **0.972±0.08** | 0.500±0.00 | 0.807±0.03 |
| AlexNet | 0.599±0.01 | 0.633±0.10 | 0.441±0.02 | 0.583±0.20 | 0.527±0.01 | 0.712±0.07 |

**Table 3.** Models' features and computing time with data augmentation.

| Model | Depth | Training Time (s) | | | Model Size |
|---|---|---|---|---|---|
| | | Diabetes | Cancer | Malaria | |
| VGG16 | 16 | 185.850±9.92 | 92.062±11.76 | 308.587±12.37 | 345 MB |
| VGG19 | 19 | 175.334±11.41 | 77.802±5.04 | 296.379±12.06 | 383 MB |
| ResNet50V2 | 50 | 336.820±24.74 | 156.820±14.90 | 485.844±22.63 | 510 MB |
| ResNet101 | 101 | 527.879±34.64 | 238.317±14.09 | 805.332±45.94 | 627 MB |
| DenseNet201 | 201 | 818.486±57.52 | 381.333±21.37 | 1233.788±31.53 | 406 MB |
| InceptionV3 | 48 | 424.050±18.65 | 210.532±19.49 | 662.135±54.83 | 476 MB |
| Xception | 71 | 311.083±19.92 | 136.887±12.43 | 447.676±16.49 | 449 MB |
| MobileNetV2 | 53 | 210.154±12.40 | 98.471±7.45 | 352.509±18.75 | 270 MB |
| EfficientNetV2B3 | 82 | 660.994±34.27 | 258.688±7.40 | 1037.483±29.00 | 369 MB |
| AlexNet | 8 | 165.710±14.34 | 69.825±4.89 | 281.498±7.29 | 212 MB |

## 4. Discussion

The results show that the models behave differently for each dataset. VGG16 and VGG19 models were the most accurate in antidiabetic classification, closely followed by MobileNet and DenseNet201. InceptionV3 was the best with the cancer dataset, again, closely followed by DenseNet201. Finally, MobileNet, DenseNet201 and InceptionV3 obtained the highest accuracy with the malaria dataset. Despite performing best on the diabetes dataset, VGG16 and VGG19 performed poorly on the other tasks. That happens because their number of layers is insufficient to classify complex compounds such as cancer and malaria inhibitors correctly. However, anti-diabetic drugs are more similar to each other, which makes them easier to classify, even for shallow models. On the other hand, MobileNet and InceptionV3 have a medium depth, which makes them suitable for some tasks. For example, both models performed well with the malaria dataset. However, their performance dropped in the other datasets. MobileNet barely achieved AUC=0.671 in the anticancer classification, and InceptionV3 AUC=0.662 in the anti-diabetic classification. This suggests that deeper models are needed for those tasks. This is the case of DenseNet201, the deepest of the models that have been evaluated. DenseNet201 was the

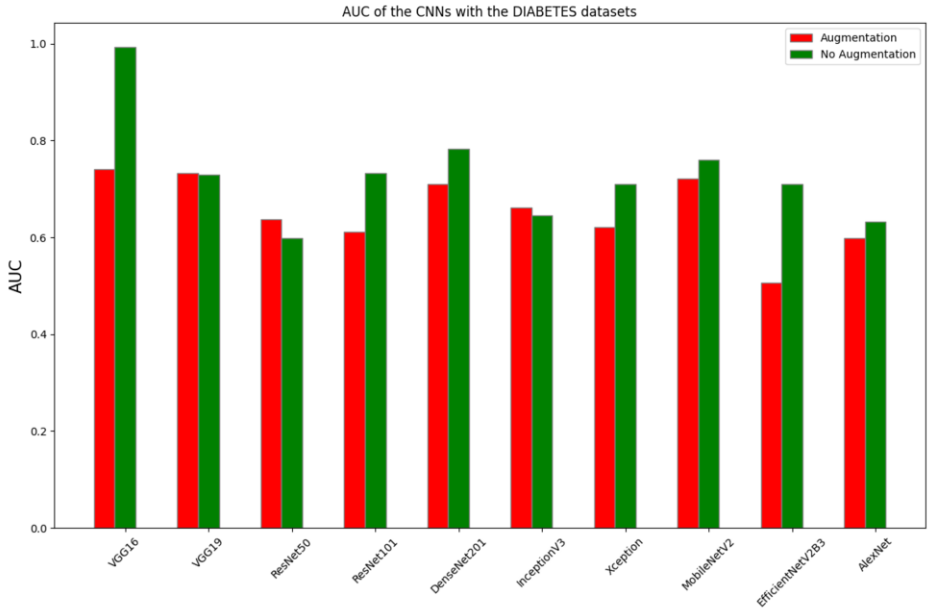


**Figure 2.** AUC comparison of the models with and without data augmentation with the Diabetes dataset.

second-best classifier in the cancer and malaria datasets, and its AUC was close to that of VGG16 in the diabetes dataset. However, the results exhibit two important limitations. First, given its high depth, it is a slow model to train (4x slower than MobileNet) and can be time-consuming with larger datasets. And secondly, although its accuracy is among the best, overall, it remains a poor model for drug classification.

On the other hand, EfficientNetV2B3 and AlexNet were demonstrated to be the least accurate models. Only in the malaria dataset did the ResNet101 model perform worse than EfficientNetV2B3 and AlexNet. AlexNet contains 8 layers, and only five of them are convolutional layers. This reduced number of convolutions may explain its low capacity to learn patterns. EfficientNetV2B3 is optimized with training-aware neural architecture search (NAS) and model scaling. These features are supposed to make it a very efficient model, although it can be less accurate than others. However, Table 3 shows that EfficientNetV2B3 is the second slowest model of our collection. This model mainly focuses on computer vision tasks, and the obtained results may indicate that it is not as effective as the other models in classification tasks.

The worryingly low quality of the models made us rethink whether data augmentation could have impacted the models' accuracy. Therefore, the models were re-trained without data augmentation. As can be seen in Figures 2, 3, and 4, the models increased their accuracy considerably in most cases. This shows that disturbing images affect the representation of compounds. For example, changing the brightness of an image causes an atom to lose some of its meaning. By varying the color, atoms of the same element with different colors become more assimilated, making it more difficult to learn the models. Another example is zooming in, which can cause certain parts of the compound to move out of the image, causing the structure of the compound to be corrupted.

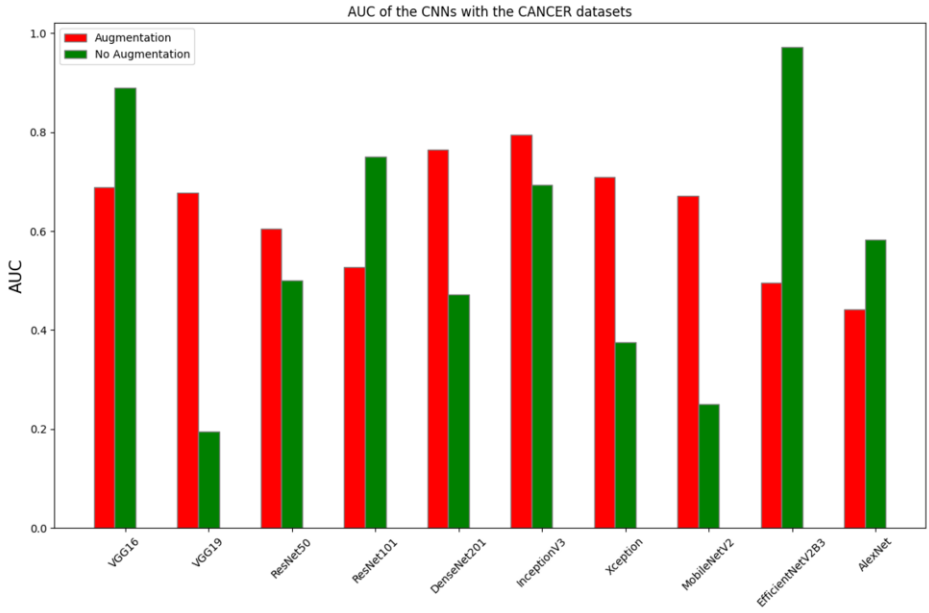


**Figure 3.** AUC comparison of the models with and without data augmentation with the Cancer dataset.

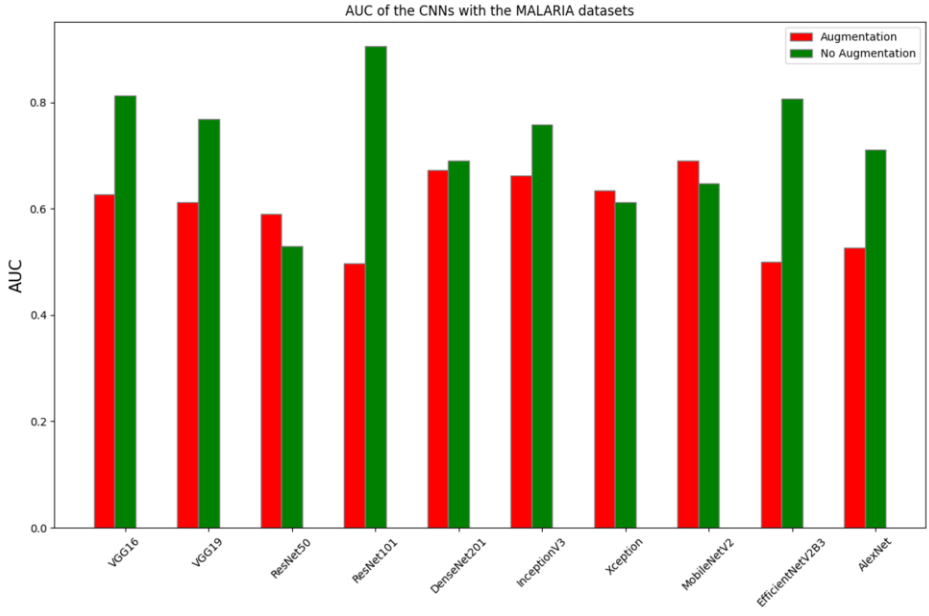


**Figure 4.** AUC comparison of the models with and without data augmentation with the Malaria dataset.

Training with the original data shows that VGG16 and EfficientNet work very well with the diabetes and malaria datasets. In addition, VGG16 also achieved the highest accuracy in the anti-diabetic dataset. Therefore, despite its shallowness, it is the model that achieves the best results. On the other hand, it is also evident that ResNet50 always predicts better with data augmentation. This indicates that this model needs many more images to be used for this type of task. The need for more images is evident in the anti-cancer dataset, as half of the models learn better with data augmentation than without. This fact is clearest in this dataset because it is clearly the smallest and, consequently, the one that needs the most images to improve.

## 5. Conclusions

Structural similarity is a way of applying virtual screening to identify, from large chemical databases, a small set of compounds that may be potential drugs. AI often assists that approach in different ways, which are related to the compounds' representation. Chemical compounds are often represented by numerical vectors or graphs. However, 2D image-based representations remain unexplored for classification purposes. CNN-based classifiers can lead to the development of GANs, which can create non-toxic synthetic drugs out of the lab. The first step towards accurate GANs is training accurate CNNs. For this purpose, ten pre-trained CNN models have been evaluated for classifying three types of drugs.

Results show that DenseNet201 outperformed the rest of the models when data augmentation was used. However, due to its high number of layers, it is a time-consuming model. Unfortunately, data augmentation perturbs the images and often modifies the structural representation of compounds. Such disturbances impair model learning. In contrast, training with the original images usually leads to better results, except for the anti-cancer dataset due to its small size. This finding demonstrates that pre-trained CNN models can serve as a basis for new classifiers of chemical compounds with certain restrictions. The first is that the images can only be altered very slightly so as not to modify the representation of the chemical structures. The second is that many images are needed for the models to learn correctly. The latter condition is often not easy to fulfill as the number of compounds labeled as drugs for a certain disease is often limited. To summarize, 2D images do not seem to be the best way of representing chemical compounds for classification tasks, but if so, no data pre-processing is strongly recommended. Instead, other representations, such as graphs, can be more effective.

Future work should investigate how to transform images without affecting performance, so that models can be trained with more data. Hyperparametrising the head layers of the classifier may also lead to improved results and is an option that needs to be explored further. It is also interesting to contrast the results with other datasets. For example, evaluating the models with fungicide and pyrethroid datasets, which are widely used in agriculture, would be an interesting application of this work in the field of environmental sciences. These compounds are found in publicly accessible chemical databases, although their identification is costly. Finally, the results obtained in this work can be compared with other representations of the compounds, like numerical vectors and graphs.

## Acknowledgments

This work has been funded by grants from the European Project Horizon 2020 SC1-BHC-02-2019 [REVERT, ID:848098]; Fundación Séneca del Centro de Coordinación de la Investigación de la Región de Murcia [Project 20988/PI/18]]; and the Spanish Ministry of Economy and Competitiveness [CTQ2017-87974-R]. Supercomputing resources in this work were supported by the Plataforma Andaluza de Bioinformática at the University of Málaga, the supercomputing infrastructure of the NLHPC (ECM-02, Powered@NLHPC), and the Extremadura Research Centre for Advanced Technologies (CETA-CIEMAT), funded by the European Regional Development Fund (ERDF). CETA-CIEMAT is part of CIEMAT and the Government of Spain.

## References

[1] Liu Q, Sun S, Rong B, Kadoch M. Intelligent reflective surface based 6G communications for sustainable energy infrastructure. IEEE Wirel Commun. 2021;28(6):49-55

[2] Rani P, Kumar R, Ahmed NMS, Jain A. A decision support system for heart disease prediction based upon machine learning. J Reliab Intell Environ. 2021;7(3):263-275

[3] Rudrapal M, Khairnar SJ, Jadhav AG. Drug repurposing (DR): an emerging approach in drug discovery. Drug repurposing-hypothesis, molecular aspects and therapeutic applications. 2020;1(1)

[4] Singh TU, Parida S, Lingaraju MC, Kesavan M, Kumar D, Singh RK. Drug repurposing approach to fight COVID-19. Pharmacol Rep. 2020;72:1479-1508

[5] Mohanty S, Al Rashid MH, Mohanty C, Swayamsiddha S. Modern computational intelligence based drug repurposing for diabetes epidemic. Diabetes & Metabolic Syndrome: Clinical Research & Reviews. 2021;15(4):102180

[6] Mtambo SE, Kumalo HM. In Silico drug repurposing of FDA-approved drugs highlighting promacta as a potential inhibitor of H7N9 influenza virus. Molecules. 2022;27(14):4515

[7] Abdelsayed M, Kort EJ, Jovinge S, Mercola M. Repurposing drugs to treat cardiovascular disease in the era of precision medicine. Nat Rev Cardiol. 2022;19(11):751-764

[8] KW To K, Cho W. Drug repurposing for cancer therapy in the era of precision medicine. Curr Mol Pharmacol. 2022;15(7):895-903

[9] Vázquez J, López M, Gibert E, Herrero E, Luque FJ. Merging ligand-based and structure-based methods in drug discovery: An overview of combined virtual screening approaches. Molecules. 2020;25(20):4723. doi: https://www.mdpi.com/1420-3049/25/20/4723

[10] Muegge I, Hu Y. How do we further enhance 2D fingerprint similarity searching for novel drug discovery? Expert Opin Drug Discov. 2022;17(11):1173–6. doi: http://dx.doi.org/10.1080/17460441.2022.2128332

[11] Zhang Z, Chen L, Zhong F, Wang D, Jiang J, Zhang S, Li X. Graph neural network approaches for drug-target interactions. Curr Opin Struc Biol. 2022;73:102327.

[12] Xiong J, Xiong Z, Chen K, Jiang H, Zheng M. Graph neural networks for automated de novo drug design. Drug Discov Today. 2021;26(6):1382-1393.

[13] Jumper J, Evans R, Pritzel A, Green T, Figurnov M, Ronneberger O, Hassabis D. Highly accurate protein structure prediction with AlphaFold. Nature. 2021;596(7873):583-589.

[14] Li H, Sze K-H, Lu G, Ballester PJ. Machine-learning scoring functions for structure-based virtual screening. Wiley Interdiscip Rev Comput Mol Sci. 2021;11(1). doi: http://dx.doi.org/10.1002/wcms.1478

[15] Tran-Nguyen V-K, Junaid M, Simeon S, Ballester PJ. A practical guide to machine-learning scoring for structure-based virtual screening. Nat Protoc. 2023;18(11):3460–511. doi: https://www.nature.com/articles/s41596-023-00885-w

[16] Qian Y, Wu J, Zhang Q. CAT-CPI: Combining CNN and transformer to learn compound image features for predicting compound-protein interactions. Front Mol Biosci. 2022;9. doi: http://dx.doi.org/10.3389/fmolb.2022.963912

[17] Hirohara M, Saito Y, Koda Y, Sato K, Sakakibara Y. Convolutional neural network based on SMILES representation of compounds for detecting chemical motif. BMC bioinformatics. 2018;19:83-94.
[18] Li C, Feng J, Liu S, Yao J. A novel molecular representation learning for molecular property prediction with a multiple SMILES-based augmentation. Computational Intelligence and Neuroscience. 2022;2022. doi: https://doi.org/10.1155/2022/8464452
[19] Mendolia I, Contino S, De Simone G, Perricone U, Pirrone R. EMBER—embedding multiple molecular fingerprints for Virtual Screening. Int J Mol Sci. 2022;23(4):2156. doi: https://www.mdpi.com/1422-0067/23/4/2156
[20] Bian Y, Xie X-Q. Generative chemistry: drug discovery with deep learning generative models. J Mol Model. 2021;27(3). doi: http://dx.doi.org/10.1007/s00894-021-04674-8
[21] Hussain S, Anees A, Das A, Nguyen BP, Marzuki M, Lin S, et al. High-content image generation for drug discovery using generative adversarial networks. Neural Netw. 2020;132:353–63. doi: http://dx.doi.org/10.1016/j.neunet.2020.09.007
[22] Tang B, Ewalt J, Ng H-L. Generative AI models for drug discovery. In: Biophysical and Computational Tools in Drug Discovery. Cham: Springer International Publishing; 2021. p. 221–43.
[23] O'Boyle NM, Banck M, James CA, Morley C, Vandermeersch T, Hutchison GR. Open Babel: An open chemical toolbox. J Cheminform. 2011;3(1). doi: http://dx.doi.org/10.1186/1758-2946-3-33
[24] Pérez-Sánchez H, den-Haan H, Peña-García J, Lozano-Sánchez J, Martínez Moreno ME, Sánchez-Pérez A, et al. DIA-DB: A database and web server for the prediction of diabetes drugs. J Chem Inf Model. 2020;60(9):4124–30. doi: http://dx.doi.org/10.1021/acs.jcim.0c00107
[25] Mswahili ME, Martin GL, Woo J, Choi GJ, Jeong Y-S. Antimalarial drug predictions using molecular descriptors and machine learning against Plasmodium falciparum. Biomolecules [Internet]. 2021;11(12):1750. doi: http://dx.doi.org/10.3390/biom11121750
[26] Nussbaumer S, Bonnabry P, Veuthey J-L, Fleury-Souverain S. Analysis of anticancer drugs: A review. Talanta. 2011;85(5):2265–89. doi: http://dx.doi.org/10.1016/j.talanta.2011.08.034
[27] Wishart DS, Feunang YD, Guo AC, Lo EJ, Marcu A, Grant JR, et al. DrugBank 5.0: a major update to the DrugBank database for 2018. Nucleic Acids Res. 2018;46(D1):D1074–82. doi: https://academic.oup.com/nar/article/46/D1/D1074/4602867?login=true
[28] Gaulton A, Hersey A, Nowotka M, Bento AP, Chambers J, Mendez D, et al. The ChEMBL database in 2017, Nucleic Acids Res. 2017;45(D1):D945–D954. doi: https://doi.org/10.1093/nar/gkw1074
[29] Russakovsky O, Deng J, Su H, et al. ImageNet Large Scale Visual Recognition Challenge. Int J Comput Vis. 2015;115(3):211-–252
[30] He K, Zhang X, Ren S, Sun J. Deep residual learning for image recognition. In: Proceedings of the IEEE conference on computer vision and pattern recognition. 2016;770–778
[31] Huang G, Liu Z, Van Der Maaten L, Weinberger KQ. Densely connected convolutional networks. In: Proceedings of the IEEE conference on computer vision and pattern recognition. 2017;4700–4708
[32] Szegedy C, Vanhoucke V, Ioffe S, Shlens J, Wojna Z. Rethinking the inception architecture for computer vision. In: Proceedings of the IEEE conference on computer vision and pattern recognition. 2016;2818–2826
[33] Chollet F. Xception: Deep learning with depthwise separable convolutions. In: Proceedings of the IEEE conference on computer vision and pattern recognition. 2017;1251–1258.
[34] Sandler M, Howard A, Zhu M, Zhmoginov A, Chen LC. Mobilenetv2: Inverted residuals and linear bottlenecks. In: Proceedings of the IEEE conference on computer vision and pattern recognition. 2018;4510–4520
[35] Tan M, Le QV. EfficientNetV2: Smaller models and faster training. arXiv. 2021. Available from: https://proceedings.mlr.press/v139/tan21a/tan21a.pdf
[36] Krizhevsky A, Sutskever I, Hinton GE. Imagenet classification with deep convolutional neural networks. Communications of the ACM. 2017;60(6):84-90. doi: https://doi.org/10.1145/3065386
[37] AlexNet_Prototype_Model. https://github.com/animikhaich/AlexNet-Tensorflow/blob/main/AlexNet_Prototype_Model.ipynb. Accessed: 26 February 2024
[38] Deng J, Dong W, Socher R, Li L-J, Li K, Fei-Fei L. ImageNet: A large-scale hierarchical image database. In: 2009 IEEE Conference on Computer Vision and Pattern Recognition. IEEE; 2009; 248-–55.
[39] Wood L, Tan Z, Stenbit I, Bischof J, Zhu S, Chollet F, Sreepathihalli D, Sampath R. KerasCV. https://keras.io/api/applications/. Accessed: 10 April 2024